Dynamics of water interacting with biomolecules

Groot, C.C.M.

Publication date
2017
Document Version
Other version
License
Other

3 Experimental methods

The results described in this thesis are obtained with pump-probe spectroscopy experiments. The experimental setup for these experiments contains three main ingredients:

- Infrared light generation: We need intense and ultrashort light pulses in the infrared spectral region. Since there are no lasers that can directly produce these pulses, the frequency of an ultrafast near-infrared laser is converted to the infrared.
- Pump-probe configuration: The infrared pulses are used as pump and probe beams, which are overlapped in the sample. The time delay between the beams can be adjusted and every other pump pulse is blocked.
- Infrared light detection: The transmitted probe light with and without pump excitation is measured by a spectrometer in combination with an infrared array detector, for a range of different pump-probe time delays. This yields the transient absorption spectrum.

In the following we first describe the principles of optical frequency conversion processes that are used to generate infrared light pulses, followed by the details of the pump-probe setups and the studied samples.

3.1 Optical frequency conversion

Light frequency conversion processes rely on the nonlinear optical response of materials. The macroscopic optical response of a material is described by the induced polarization $\vec{P}$, which is the dipole moment per unit volume. $\vec{P}$ can be written as a power series of the applied electric field $\vec{E}$:

$$\vec{P}(t) = \epsilon_0[\chi^{(1)}\vec{E}(t) + \chi^{(2)}\vec{E}(t)^2 + \chi^{(3)}\vec{E}(t)^3 + ...\chi^{(n)}\vec{E}(t)^n] \tag{3.1}$$

where $\chi^{(n)}$ is known as the n^{th}-order optical susceptibility. In contrast to the nonlinear response mentioned in the previous chapter, we have assumed here that we are far away from any resonance. This means that no light is absorbed and that the polarization response is instantaneous, i.e. following the momentary sources. Most materials that are illuminated by everyday (weak) light are fully described by the first term of eq. 3.1, the linear response. Typically, only lasers produce high enough electric fields to induce a higher order polarization response. To illustrate how a nonlinear optical response leads to frequency conversion, we consider a planar electric field moving in direction $\vec{x}$ with two distinct frequency components ω_1 and ω_2:

$$\vec{E}(\vec{x},t) = \vec{E}_1 e^{i(\vec{k}_1\vec{x}-\omega_1 t)} + \vec{E}_2 e^{i(\vec{k}_2\vec{x}-\omega_2 t)} + c.c. \tag{3.2}$$

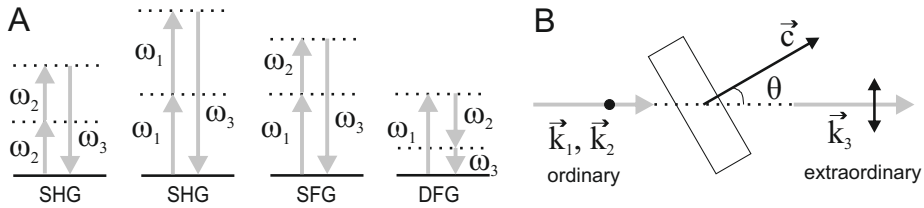

FIGURE 3.1. (A) Energy level description of second-order frequency conversion processes induced by light fields at ω_1 and ω_2: second harmonic generation (SHG), sum-frequency generation (SFG) and difference-frequency generation (DFG). Dashed lines indicate virtual states. (B) Geometry of phase-matching for sum-frequency generation in a negative ($n_e < n_o$) uniaxial crystal (type I). The dot and double-sided arrow indicate the polarization directions of the fields.

The second-order polarization response is then given by[70]

$$\vec{P}^{(2)}(\vec{x},t) = \epsilon_0 \chi^{(2)} \vec{E}(\vec{x},t)^2 \tag{3.3}$$

$$\begin{aligned} \vec{E}(\vec{x},t)^2 =& \vec{E}_1^2 e^{i(2\vec{k}_1\vec{x}-2\omega_1 t)} + c.c. && (SHG) \\ &+ \vec{E}_2^2 e^{i(2\vec{k}_2\vec{x}-2\omega_2 t)} + c.c. && (SHG) \\ &+ 2\vec{E}_1 \cdot \vec{E}_2 e^{i((\vec{k}_1+\vec{k}_2)\vec{x}-(\omega_1+\omega_2)t)} + c.c. && (SFG) \\ &+ 2\vec{E}_1 \cdot \vec{E}_2^* e^{i((\vec{k}_1-\vec{k}_2)\vec{x}-(\omega_1-\omega_2)t)} + c.c. && (DFG) \\ &+ 2|\vec{E}_1|^2 + 2|\vec{E}_2|^2 && (OR) \end{aligned} \tag{3.4}$$

The second-order polarization response contains terms with different combinations of the input frequencies ω_1 and ω_2: these correspond to the processes of frequency doubling, or second harmonic generation (SHG), sum-frequency generation (SFG), difference-frequency generation (DFG) and optical rectification (OR). These processes are illustrated in fig. 3.1A.

The efficiency of each conversion process depends on the so-called phase-matching condition. Both the input fields and generated field travel through the material at a speed given by their wavevector $\vec{k}$, where $\vec{k} = \vec{n}\omega/c$, with $\vec{n}$ the refractive index of the medium and c the speed of light. To get efficient conversion, the generated field at any point in the material must maintain a fixed phase relation with respect to the field generated earlier. Microscopically this means that the individual atomic dipoles of the material all are phased such that the field emitted by each dipole adds up constructively in the propagation direction of the field. This is the case when the following condition is fulfilled:

$$\sum \vec{k}_- = \sum \vec{k}_+ \tag{3.5}$$

where $\vec{k}_-$ and $\vec{k}_+$ refer to the wavevector(s) of the converted fields (upward arrows in fig. 3.1) and generated fields (downward arrows), respectively. In practice, phase matching is not so easy to achieve. To illustrate this, we consider

the case of sum-frequency generation, for which eq. 3.5 reduces to

$$\vec{k}_1 + \vec{k}_2 = \vec{k}_3 \tag{3.6}$$

or equivalently,

$$\vec{n}_1\omega_1 + \vec{n}_2\omega_2 = \vec{n}_3\omega_3 \tag{3.7}$$

Since for most materials the refractive index $\vec{n}$ increases with frequency, the right side of eq. 3.7 is almost always larger than the left side. A common way to solve this problem is by using birefringent crystals. The refractive index of birefringent materials depends on the polarization direction of the light. Thus the phase-matching condition can be fulfilled by a proper choice of the polarization of the input fields and the orientation of the crystal. Consider for example the case of sum-frequency generation in a uniaxial crystal illustrated in fig. 3.1B. Here the two input fields are polarized perpendicular to the plane containing their wavevector $\vec{k}$ and the optical axis $\vec{c}$ of the crystal, making them experience the so-called ordinary refractive index n_o, while the generated field is polarized in the plane spanned by $\vec{k}$ and $\vec{c}$, so it experiences the so-called extraordinary refractive index $n_e(\theta)$:

$$\frac{1}{{n_e}^2(\theta)} = \frac{\cos^2\theta}{{n_o}^2} + \frac{\sin^2\theta}{{n_e}^2} \tag{3.8}$$

The extraordinary index depends on the angle θ between $\vec{k}$ and $\vec{c}$, which makes it possible to fulfill the phase-matching condition of eq. 3.7 by choosing the appropriate angle θ. In general, depending on the type of second-order process and the crystal material, different polarization combinations can be used to acquire phase matching.

For time-resolved spectroscopy, light needs to be pulsed, and pulses are inherently not monochromatic but span a range of frequencies. In this case the phase-matching condition cannot be perfectly fulfilled for all frequencies in the pulse: at the edges of the pulse spectrum the conversion efficiency decreases, which can lead to a narrowing of the generated pulse spectrum and consequently an increase in pulse duration. For undepleted input fields, the generated intensity depends on the wavevector mismatch $\Delta\vec{k} = \sum \vec{k}_+ - \sum \vec{k}_-$ and the crystal thickness L:

$$I(\omega) = I_0 \,\mathrm{sinc}^2(\Delta\vec{k}(\omega)L/2) \tag{3.9}$$

The above equation shows that it is possible to achieve a higher phase matching bandwidth - meaning a higher range of $\Delta\vec{k}$ for which $I > \frac{1}{2}I_0$ - by choosing a thinner crystal (smaller L). Of course, a thinner crystal also lowers the maximum generated intensity, so an optimal crystal length must be used based on the desired spectrum, duration and intensity of the generated pulse.

OPTICAL PARAMETRIC AMPLIFICATION A specific case of difference-frequency generation is optical parametric amplification (OPA). In this case the input fields are an intense high frequency beam, called the pump, and a very weak seed beam of lower frequency ω_s. During the OPA process, the weak seed

beam is amplified. In addition a new beam is created at the frequency ω_i, with $\omega_p = \omega_s + \omega_i$. The amplified beam is called the signal and the new beam is called the idler. Usually, the weak seed beam is chosen to be broadband white light; due to the broad bandwidth, the frequencies of the amplified signal and generated idler beams mostly depend on the phase-matching condition, and can be tuned over a wide range by changing the OPA crystal angle.

3.2 Single-color infrared pump-probe setup

The single-color infrared pump-probe setup used to obtain many results described later in this thesis is shown schematically in fig. 3.2. A Ti:sapphire regenerative amplifier (Spectra-Physics Hurricane) produces 900 μJ, 100 femtosecond pulses with a central wavelength of 800 nm at a repetition rate of 1 kHz. Part of this light is used to pump a β-bariumborate (BBO)-based optical parametric amplifier (OPA, Spectra-physics). In the OPA, a small part of the 800 nm light is focused into a sapphire plate to generate a broadband white light seed, which is amplified in two steps to generate signal and idler pulses of 1.33 μm and 2 μm respectively. The idler pulses are frequency-doubled in another BBO crystal and subsequently mixed with the remaining 800 nm light in a lithiumniobate (LN) crystal to produce 10 μJ infrared pulses centered at 2500 cm^{-1}, with a bandwidth of 100 cm^{-1} and a pulse duration of 200 fs. To ensure that no other light enters the pump-probe experiment, two long wave pass filters (one after the OPA, another after the DFG stage) filter out the remaining 800 nm light, and a germanium plate after the DFG stage filters out the signal and idler beams.

The polarization of the infrared pulses is cleaned up by a polarizer and the pulses are split into pump, probe and reference beams by a wedged CaF_2 window. The pump pulse passes through a $\lambda/2$ plate to rotate the pump polarization by 45°, and is chopped at 500 Hz to block every other pulse. The probe pulse passes over a motorized delay stage. All three beams are focused into the sample by a gold-coated parabolic mirror (focal length f=100 mm). The pump and probe beams are spatially overlapped in the sample, such that the probe beam monitors the pump-induced absorption changes, while the reference beam is focused at a different spot and used to correct for pulse-to-pulse intensity fluctuations of the probe. A rotating polarizer, placed directly after the sample, selects probe and reference pulses that are polarized either parallel or perpendicular with respect to the pump polarization. After passing through the sample and rotating polarizer, the probe and reference beams are recollimated using a second parabolic mirror, sent to a grating-based spectrometer (Lot Oriel MSH302) and detected by a 3x32 mercury-cadmium-telluride (MCT) array.

In some of the experiments, a wobbler is placed into the pump path to suppress the undesired interference effects in the signal due to scattering of the pump beam into the probe detector path[71]. The wobbler consists of a CaF_2 plate at Brewster angle that is slightly rotated at a frequency of 250 Hz using a set of electromagnets. By setting the correct phase and amplitude of the

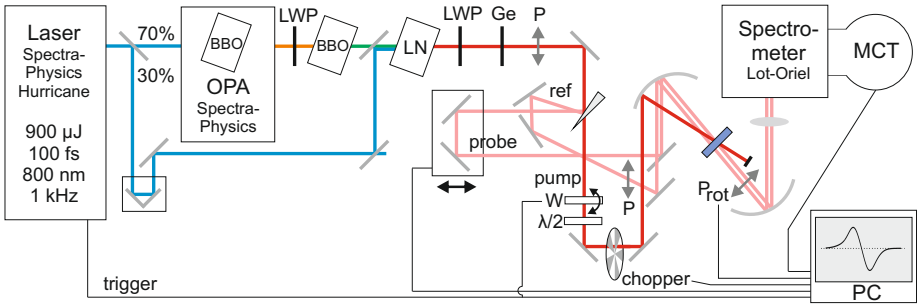

FIGURE 3.2. Schematic of the single-color pump-probe setup described in the text (not to scale). BBO: β-bariumborate crystal, LN: lithiumniobate crystal, LWP: long wave pass filter, Ge: Germanium filter, P: polarizer, P_{rot}: rotating polarizer, W: wobbler (optional), $\lambda/2$: half-wave plate, MCT: Mercury-Cadmium-Telluride detector. The colored lines indicate light beams, while the thin black lines indicate electronic signals.

rotation (via the voltage applied to the electromagnets), the pump phase can be modulated such that the unwanted interference signals average out.

3.3 DUAL-COLOR (2D) INFRARED PUMP-PROBE SETUP

The dual-color infrared pump-probe setup used for some of the experiments described in this thesis is shown schematically in fig. 3.3. It can be used in pump-probe mode, or in 2D mode by passing the pump beam through an interferometer.

A Ti:sapphire regenerative amplifier (Coherent) produces 3.3 mJ, 35 femtosecond pulses with a central wavelength of 800 nm at a repetition rate of 1 kHz. The main part of this light is used to generate the pump beam. Firstly, a white-light-seeded, three-step, β-bariumborate (BBO)-based OPA (Spectra-Physics) generates signal and idler pulses that are tunable between 1.1-1.6 μm and 1.6-2.9 μm respectively. The signal and idler pulses are difference-frequency mixed in a silver gallium disulfide ($AgGaS_2$) crystal to produce infrared pump pulses that are tunable between 1500 and 4000 cm^{-1}, with typical energies of 20 μJ, a bandwidth of 300 cm^{-1} (FWHM) and a pulse duration of 170 fs. The pump pulse passes through a $\lambda/2$ plate to rotate the pump polarization by 45°, and is then chopped at 500 Hz to block every other pulse. The probe and reference beams are generated using a similar conversion scheme: a two-step, white-light-seeded, BBO-based OPA (home-build) generates signal and idler pulses that are difference-frequency mixed in a $AgGaS_2$ crystal. This produces 4 μJ infrared pulses tunable from 1500 to 4000 cm^{-1}, with a bandwidth of 320 cm^{-1} (FWHM) and a pulse duration of 170 fs. The generated infrared light is sent through a germanium plate that blocks the signal and idler light,

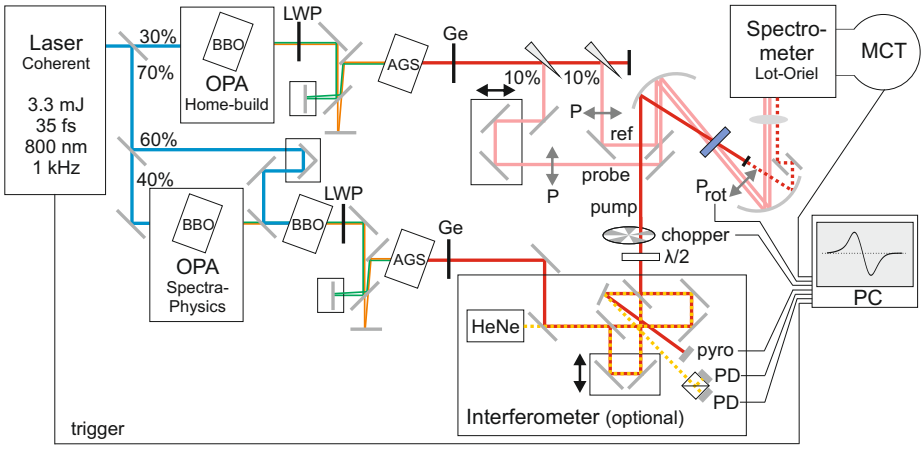

FIGURE 3.3. Schematic of the dual-color pump-probe setup described in the text (not to scale). BBO: β-bariumborate crystal, AGS: silver gallium disulfide ($AgGaS_2$) crystal, LWP: long wave pass filter, Ge: Germanium filter, P: polarizer, P_{rot}: rotating polarizer, $\lambda/2$: half-wave plate, HeNe: helium-neon laser, pyro: pyroelectric detector, PD: photodiode, MCT: Mercury-Cadmium-Telluride detector. The colored lines indicate light beams, while the thin black lines indicate electronic signals.

and reflected off two ZnSe wedges to generate probe and reference beams. The probe beam passes through a motorized delay stage, and the polarization of both probe and reference beams is cleaned up by polarizers.

Pump, probe and reference beams are focused into the sample by a gold-coated parabolic mirror (focal length f=150 mm). The pump and probe beams are spatially overlapped in the sample, so that the probe beam monitors the pump-induced absorption changes, while the reference beam is focused at a different spot. The reference is used to correct for pulse-to-pulse intensity fluctuations of the probe. A rotating polarizer, placed directly after the sample, selects probe pulses that are polarized either parallel or perpendicular with respect to the pump polarization. After passing through the sample and rotating polarizer, the pump, probe and reference beams are recollimated using a second parabolic mirror (f=100 mm), sent to a grating-based spectrometer (Lot Oriel) and detected by a 3x32 mercury-cadmium-telluride (MCT) array. The pump beam is only passed to the detector during experimental tuning and is blocked during the actual pump-probe experiment.

2D SPECTRA To obtain two-dimensional spectra, the pump pulses can be sent through a compact Mach-Zehnder interferometer[60,72]. The interferometer produces pulse pairs with variable time delay. A reference helium-neon (HeNe) laser travels a few centimeters above the infrared beam and is detected by a quadrature counter, consisting of a $\lambda/4$ plate in one of the interferometer arms and a polarizing beam splitter and two photodiodes in the output arm. This allows for an accurate determination of the interferometer delay, even when the

delay is scanned very fast. Separate beamsplitters, placed on top of each other, are used for the infrared and HeNe light. The pump interference that results from scanning the delay is directly recorded by a pyroelectric detector in one of the output arms of the interferometer, which yields the relative phase needed to calculate the 2D spectra.

3.4 SAMPLE CELL

The liquid samples under study in this thesis are held by a sample cell that consists of two infrared-transparent windows (CaF_2 or z-cut sapphire) that are separated by a 10 to 500 μm teflon spacer. CaF_2 has the advantage of being transparent down to low frequencies: it starts absorbing below 1250 cm^{-1} while sapphire absorbs below 2300 cm^{-1}. However, sapphire is much stronger, which prevents scratching and subsequent scattering of pump light into the probe detection path. The windows and liquid are held together by a 1 inch diameter aluminum cell. This cell can in turn be mounted on a temperature-controlled stage. The stage temperature is controlled by an active feedback system that consists of two water-cooled Peltier elements, a thermocouple attached to the sample cell, and a control unit (TE Technology). Alternatively, the aluminum cell can be mounted on a rotating stage, which prevents accumulated local heating of the sample.

ISOTOPICALLY DILUTED WATER The aqueous samples under study in this thesis often contain isotopically diluted water. Isotopically diluting water means mixing normal water, H_2O, with heavy water, D_2O, which has two deuterium atoms instead of hydrogen. The hydrogen and deuterium atoms exchange due to the self-ionization of water, resulting in a near-statistical mixture of HDO, H_2O and D_2O molecules[73]. Looking at isotopically diluted water has two main advantages:

- The two hydroxyl stretch vibrations of HDO are decoupled. As a consequence, there is no splitting of the water hydroxyl stretch vibration into antisymmetric and symmetric modes.
- The concentration of OD (or OH) oscillators is very low. As a consequence, intermolecular Förster energy transfer becomes negligible. In addition, the absorption per volume is smaller, so the sample thickness can be more practical (>10 μm) and the effect of sample heating is reduced since less vibrations are excited per volume.

The absence of spectral splitting and intra- and intermolecular coupling for HDO means that the interpretation of spectra is simplified: the spectrum of the hydroxyl stretch vibration directly reflects the hydrogen-bond strength, and the anisotropy measured by a polarization-resolved pump-probe experiment directly decays with the rate of molecular reorientation.

Most experiments probe the OD stretch vibration of a few percent of HDO in H_2O. The advantage of probing the OD vibration is that the vibrational

lifetime is longer compared to the OH vibration, and that most of the sample is still H_2O, which is closer to the natural situation. A disadvantage is that there is considerable background absorption of the OH stretch in the OD spectral region, so the concentration of HDO in H_2O cannot be too low (generally it is chosen to be above 4%).